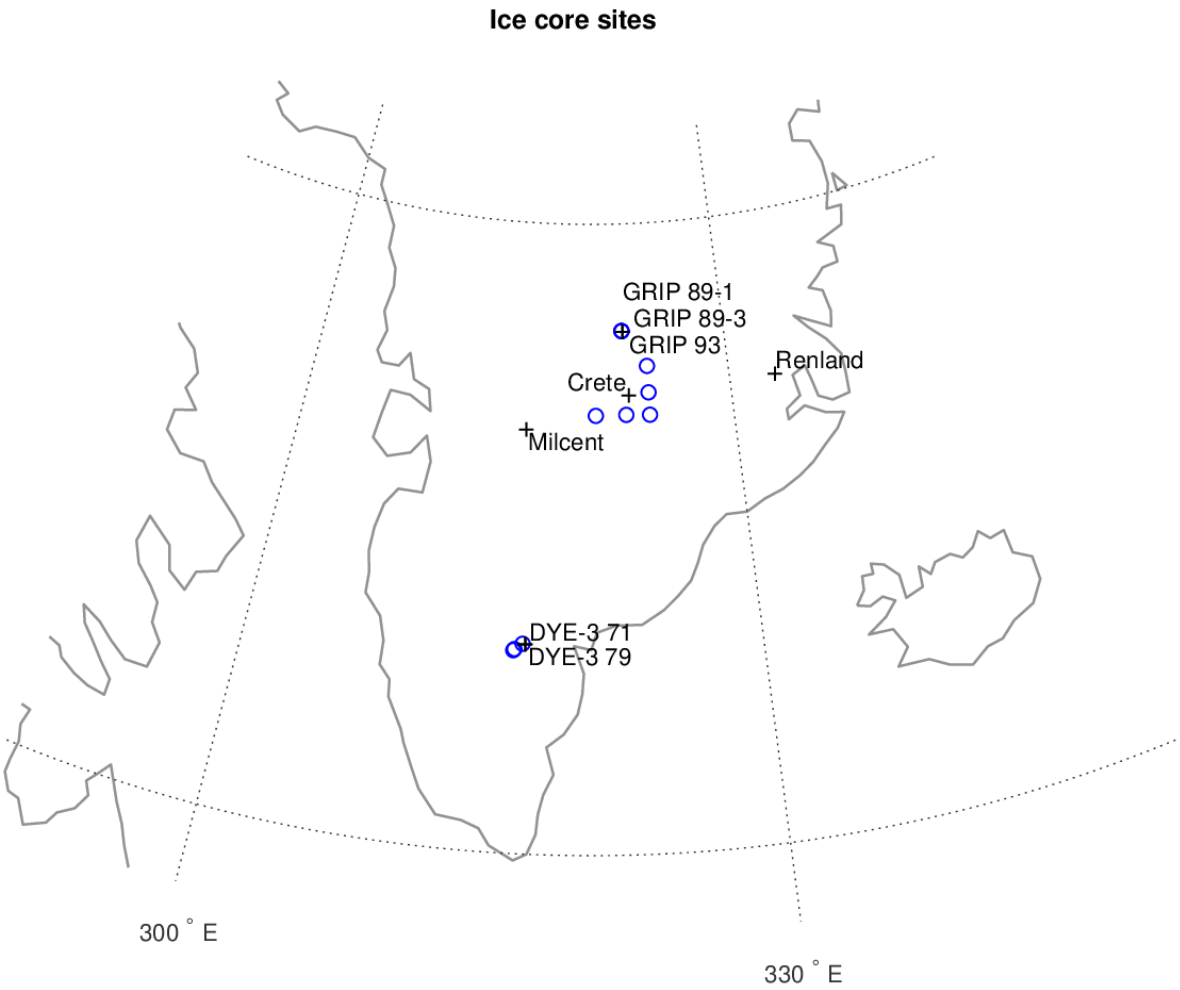

Figure S1: Locations of sites for the 8 ice cores for the period 1241-1970 (black) and the 19 cores covering 1778-1970 (blue). The 19 cores include a total of 5 cores from DYE-3 and 6 cores from GRIP, as well as Site A, B, D, E and G located close to Crete.

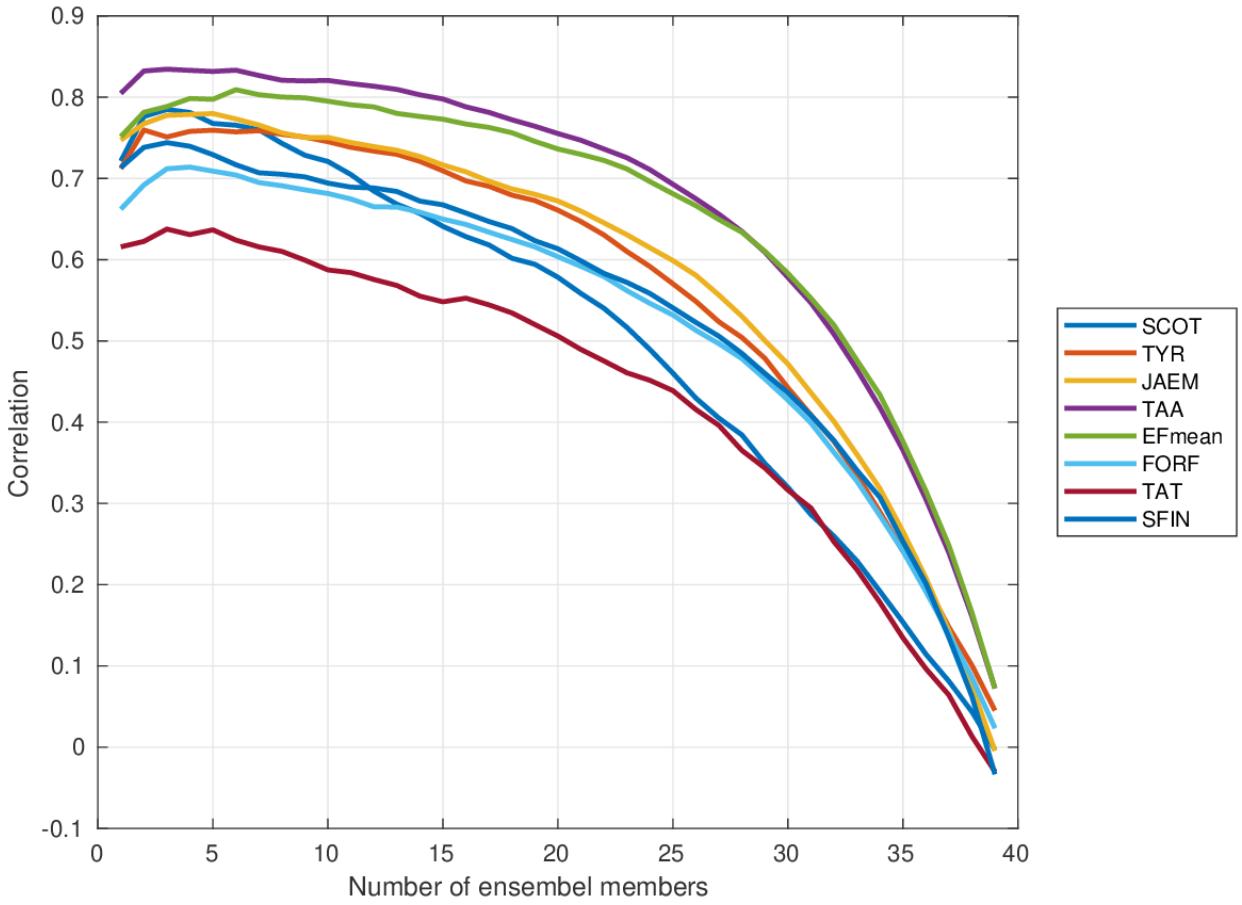

Figure S2: Correlation of reconstructed temperature for each tree ring site using increasing number of ensemble members.

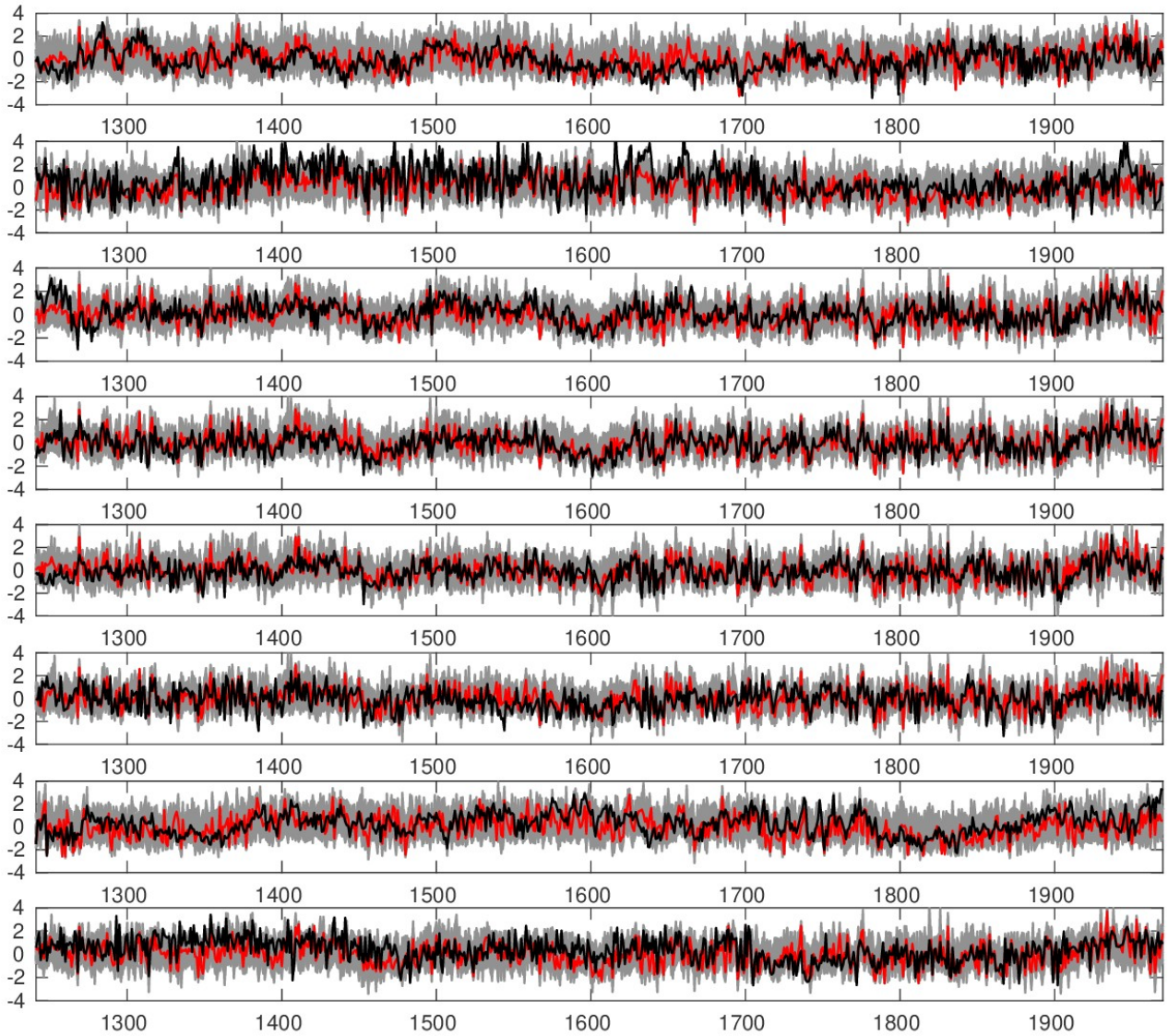

Figure S3: Comparison of reconstructed T2m at the tree ring sites with the tree ring data (black). The ensemble mean for 20 ensemble members is shown in red and all ensemble members are plotted in gray to show the spread. All data is normalized. The sites are (top to bottom): SCOT, TYR, JAEM, TAA, Efmean, FORF, TAT and SFIN.

Supplementary of Sjolte et al. CPD

Sum50 , 8 ice cores

Win50, 8 ice cores

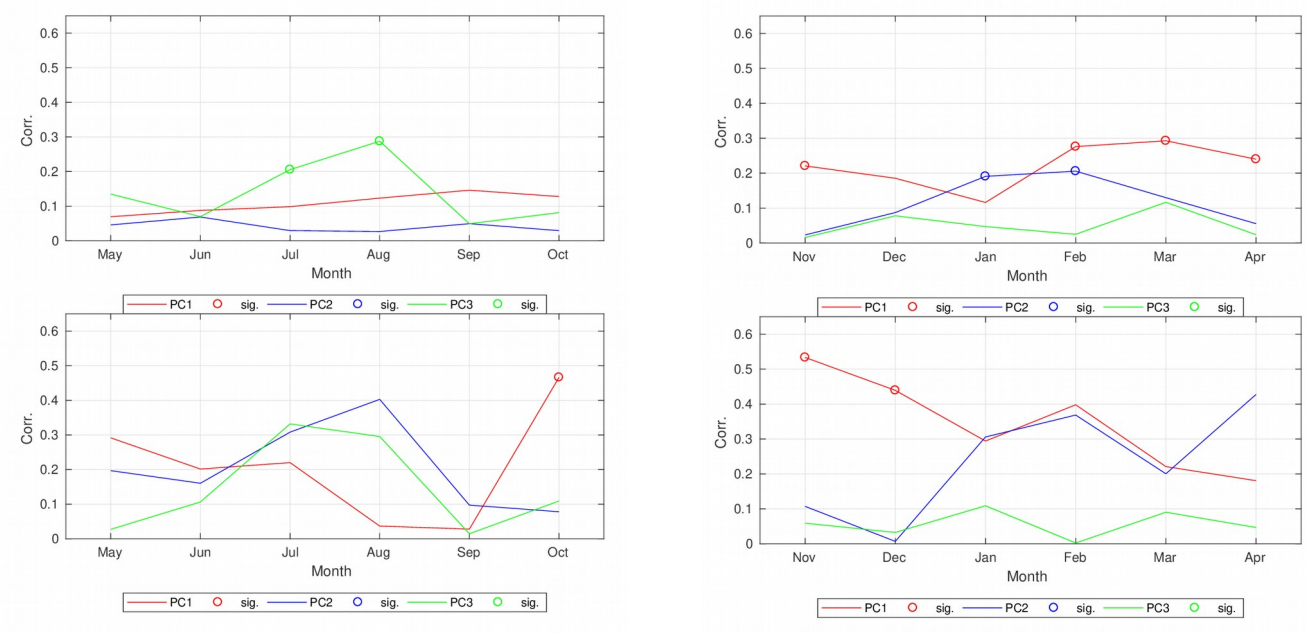

Win100, 8 ice cores

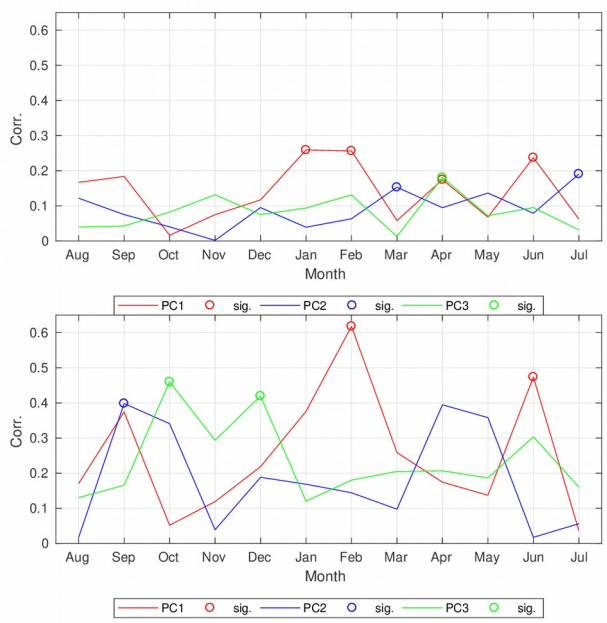

Figure S4: Test of monthly reconstructions based on 8 ice cores for sum50, win50 and win100. The first three PCs of reconstructed SLP are correlated against the PCs of 20CR SLP. The upper panel of each of the three subplots is for annual data, while the lower panel is for decadally filtered data. Circular markers indicate $p < 0.05$.

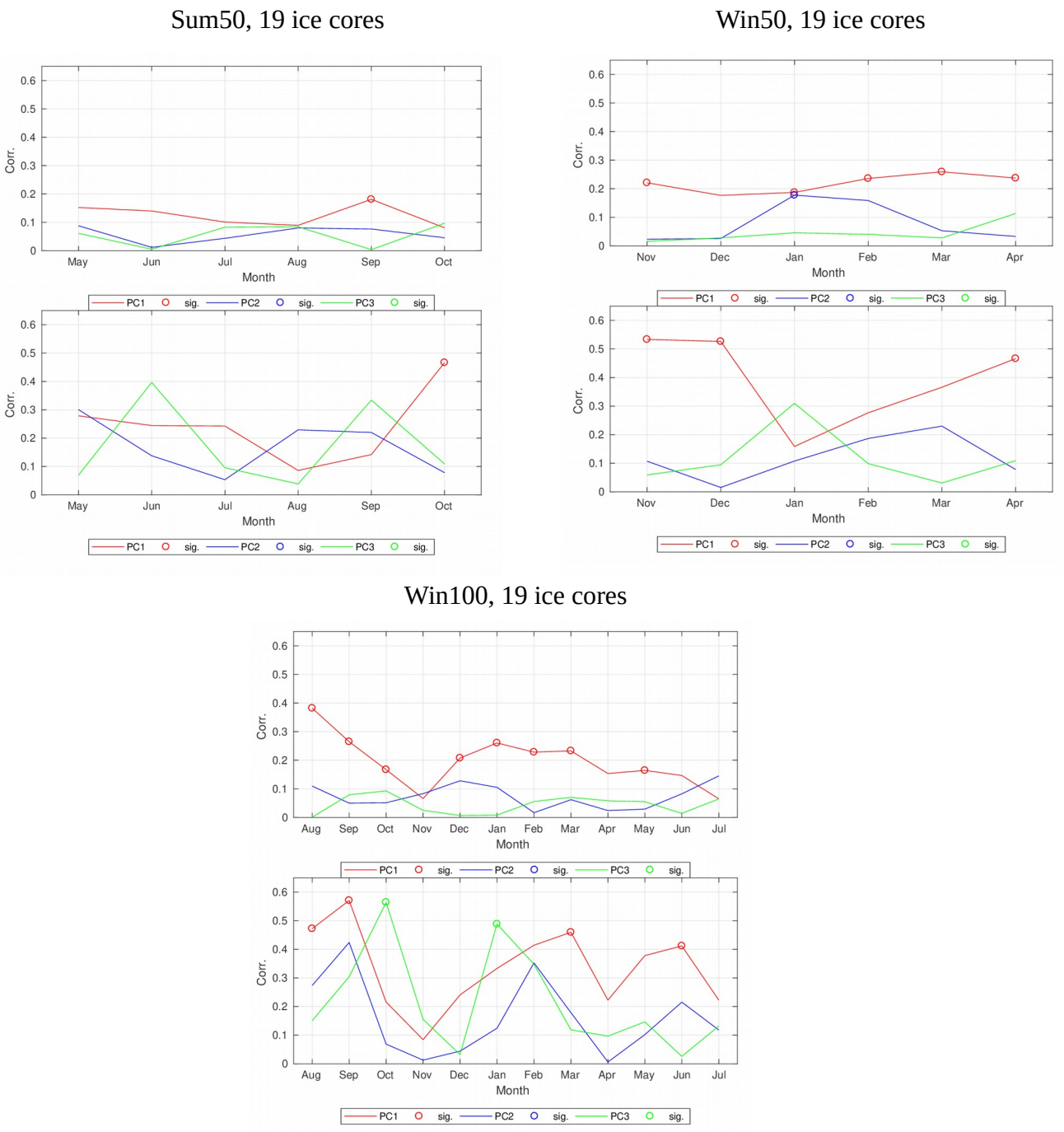

Figure S5: Test of monthly reconstructions based on 19 ice cores for sum50, win50 and win100. The first three PCs of reconstructed SLP are correlated against the PCs of 20CR SLP. The upper panel of each of the three subplots is for annual data, while the lower panel is for decadally filtered data. Circular markers indicate $p < 0.05$.

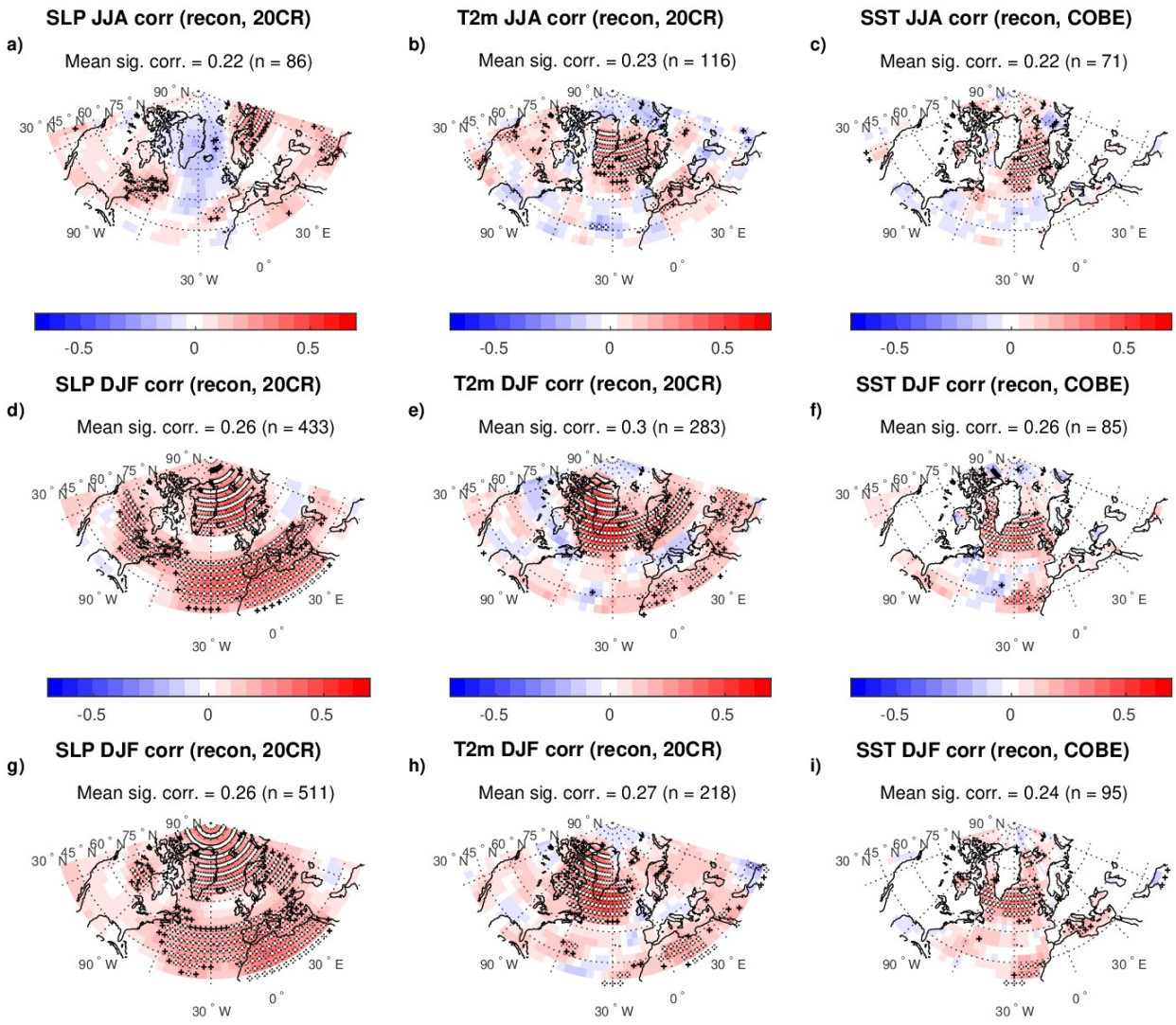

Figure S6: (**a-c**) Correlation between reconstructed (19 ice cores) and reanalysis SLP, T2m and COBE SST for JJA. The reanalysis data has been interpolated to the model grid (3.75 x 3.75 degrees). Black markers indicated $p<0.05$ and white markers indicate $p<0.025$. Also indicated is the mean correlation of all significantly correlated grid points (Mean sig. Corr.) ($p<0.05$) and the number of significant grid points (n). (**d-f**) same as a-c, but for DJF. (**g-i**) same as a-c but for DJF reconstructed from the winter centered annual mean ice core data.

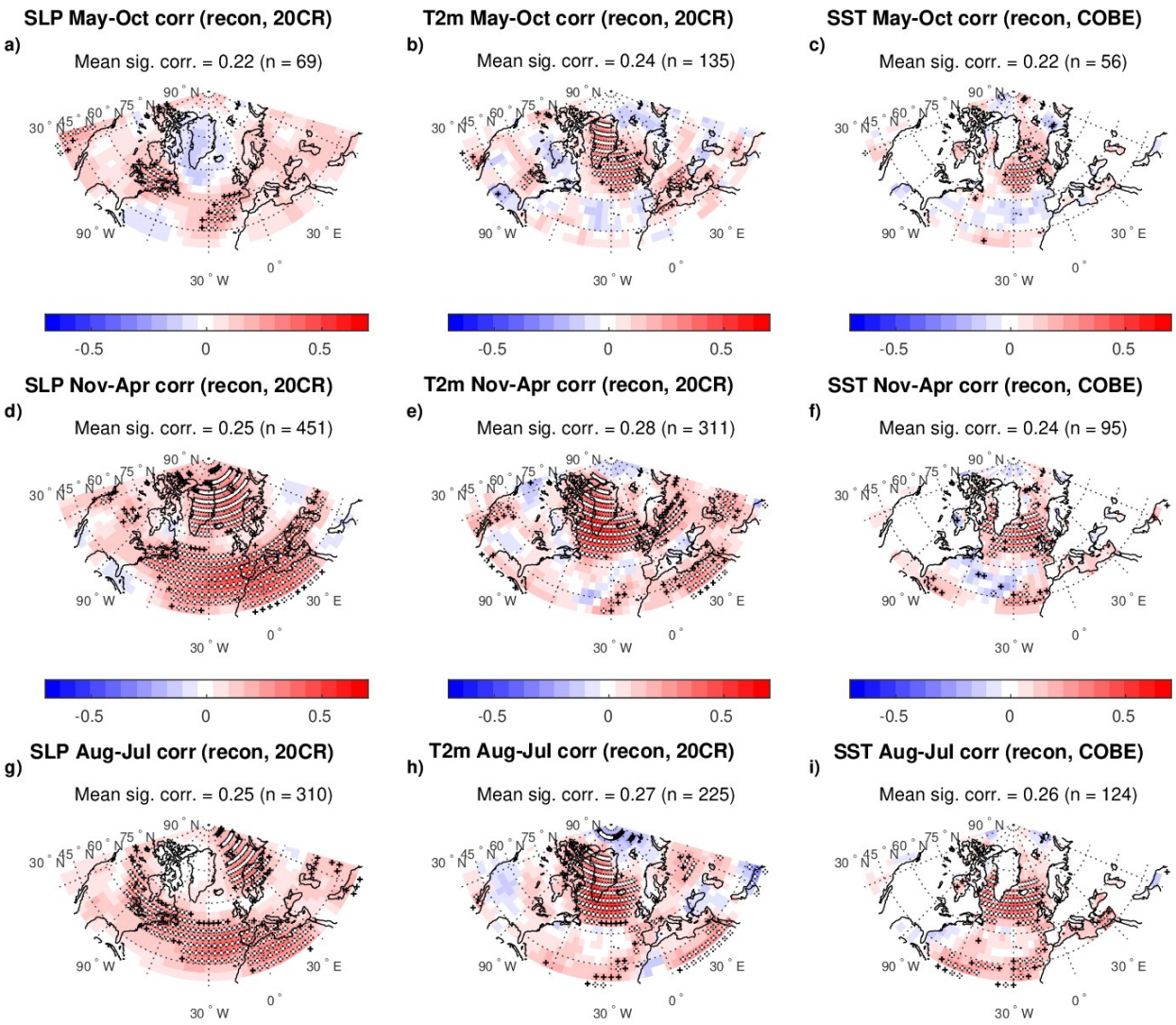

Figure S7: (**a-c**) Correlation between reconstructed (19 ice cores) and reanalysis SLP, T2m and COBE SST for sum50 (May-Oct). The reanalysis data has been interpolated to the model grid (3.75 x 3.75 degrees). Black markers indicated $p<0.05$ and white markers indicate $p<0.025$. Also indicated is the mean correlation of all significantly correlated grid points (Mean sig. Corr.) ($p<0.05$) and the number of significant grid points (n). (**d-f**) same as a-c, but for Win50 (Nov-Apr). Bottom row: same as top row, but for the winter centered annual mean (Win100, Aug-Jul).

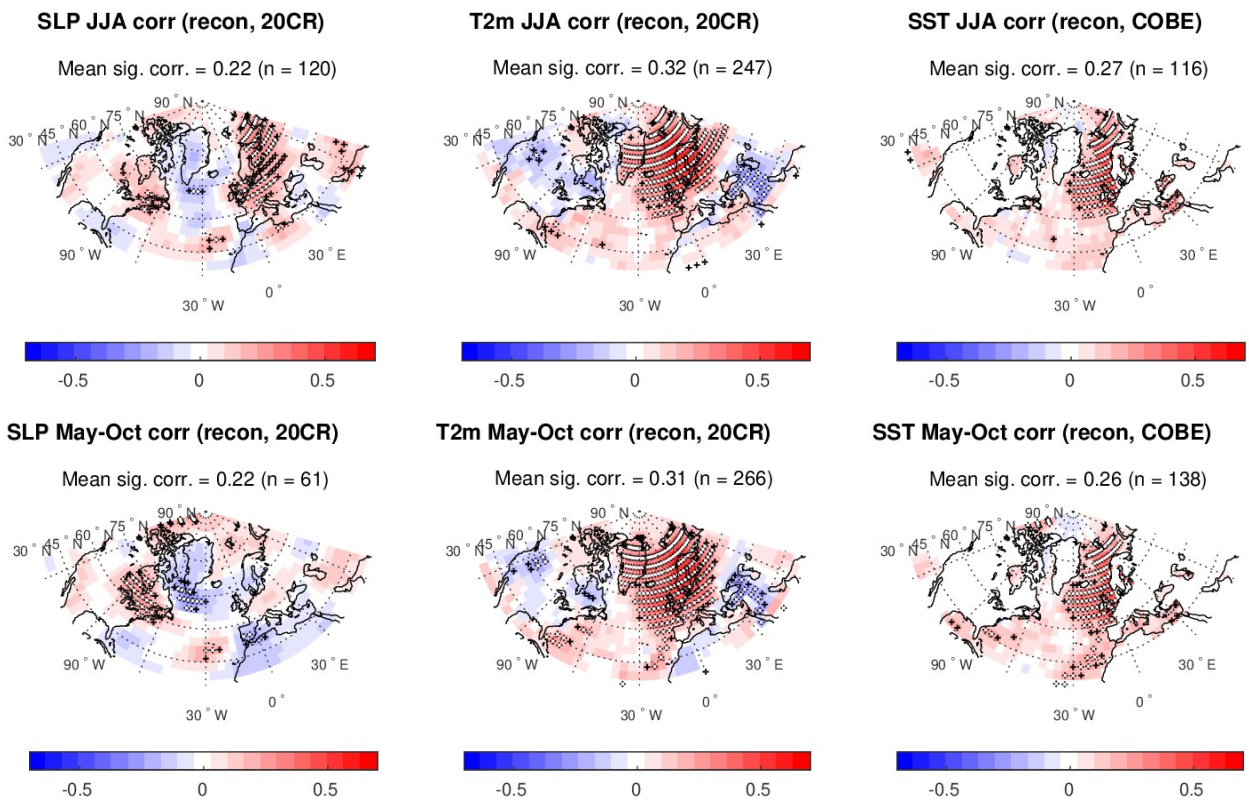

Figure S8: Top row: Correlation between reconstructed and reanalysis SLP, T2m and COBE SST for JJA constrained by tree ring data. The reanalysis data has been interpolated to the model grid (3.75 x 3.75 degrees). Black markers indicated $p<0.05$ and white markers indicate $p<0.025$. Also indicated is the mean correlation of all significantly correlated grid points (Mean sig. Corr.) ($p<0.05$) and the number of significant grid points (n). Bottom row: same as top row, but for sum50 (May-Oct).

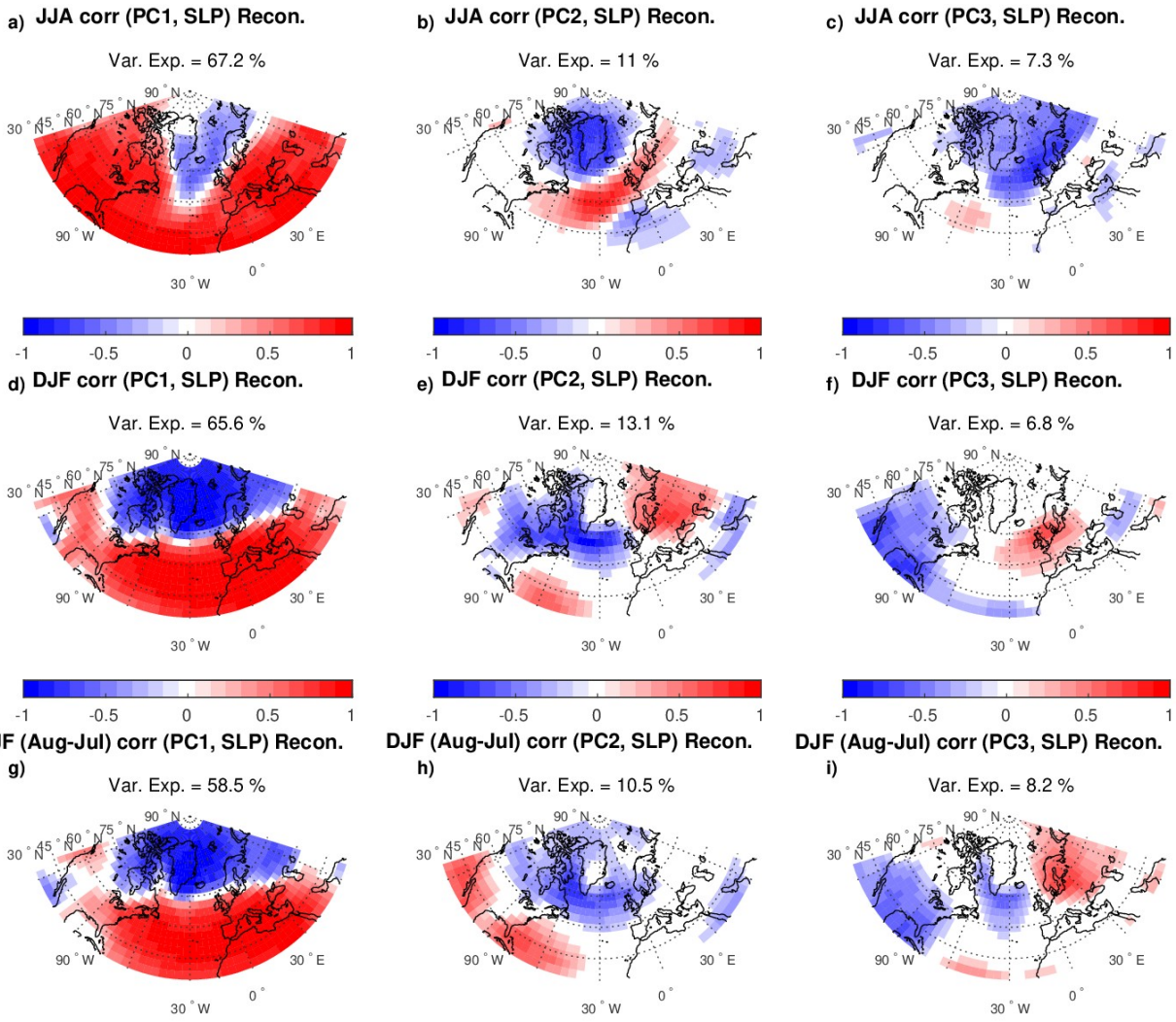

Figure S9: a)-c) regression of the first three reconstructed PCs of SLP on reconstructed (8 ice cores) JJA SLP, which corresponds to the reconstructed EOF patterns. d)-f) same as a)-c), but for DJF. g)-i) same as a)-c), but for DJF reconstructed (8 ice cores) from the winter centered annual mean ice core data. The time period is 1851-1970. Only data shown for $p<0.05$.

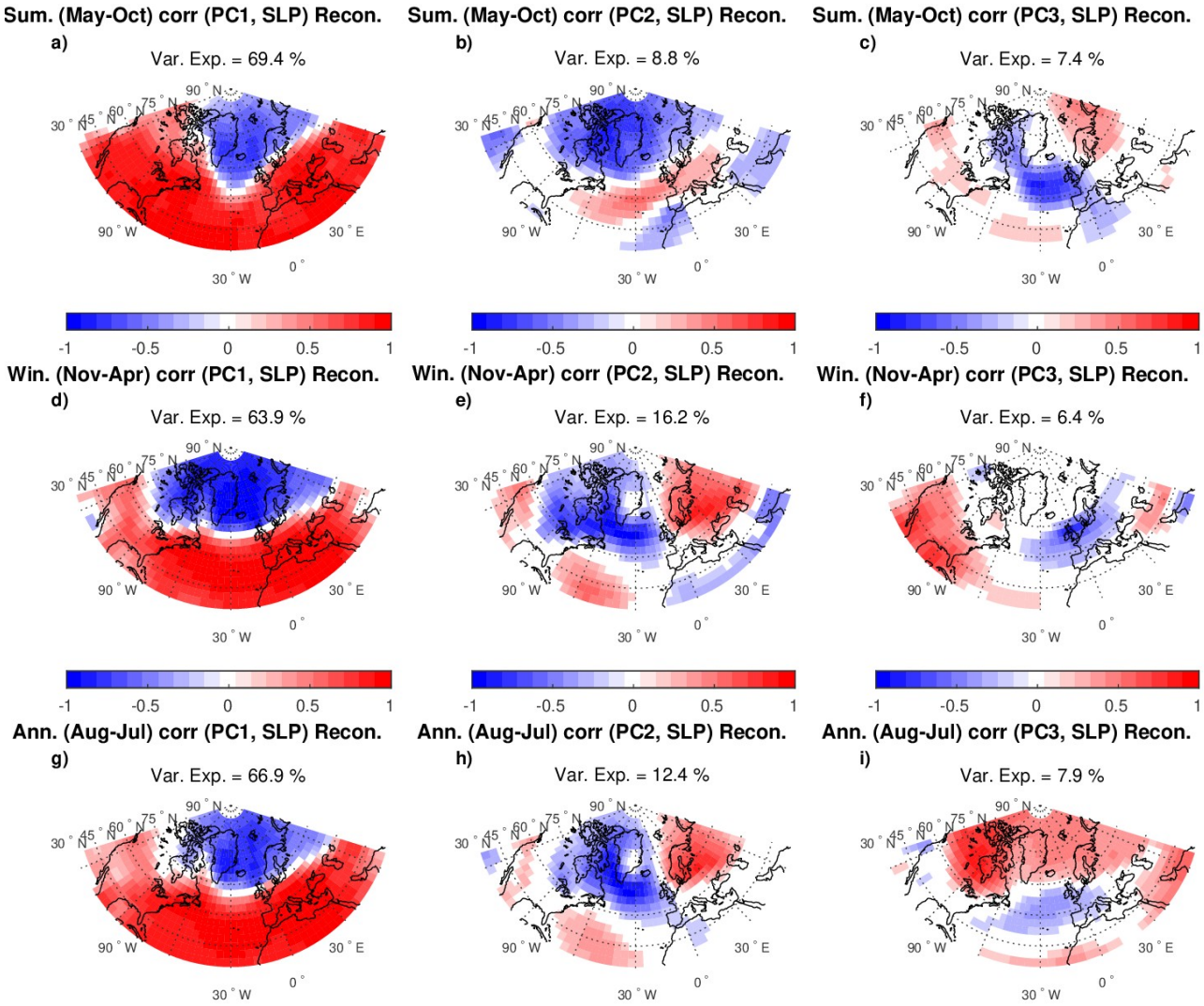

Figure S10: a)-c) regression of the first three reconstructed PCs of SLP on reconstructed (8 ice cores) Sum50 SLP, which corresponds to the reconstructed EOF patterns. d)-f) same as a)-c), but for Win50. g)-i) same as a)-c), but for the winter centered annual mean (Win100). The time period is 1851-1970. Only data shown for $p<0.05$.

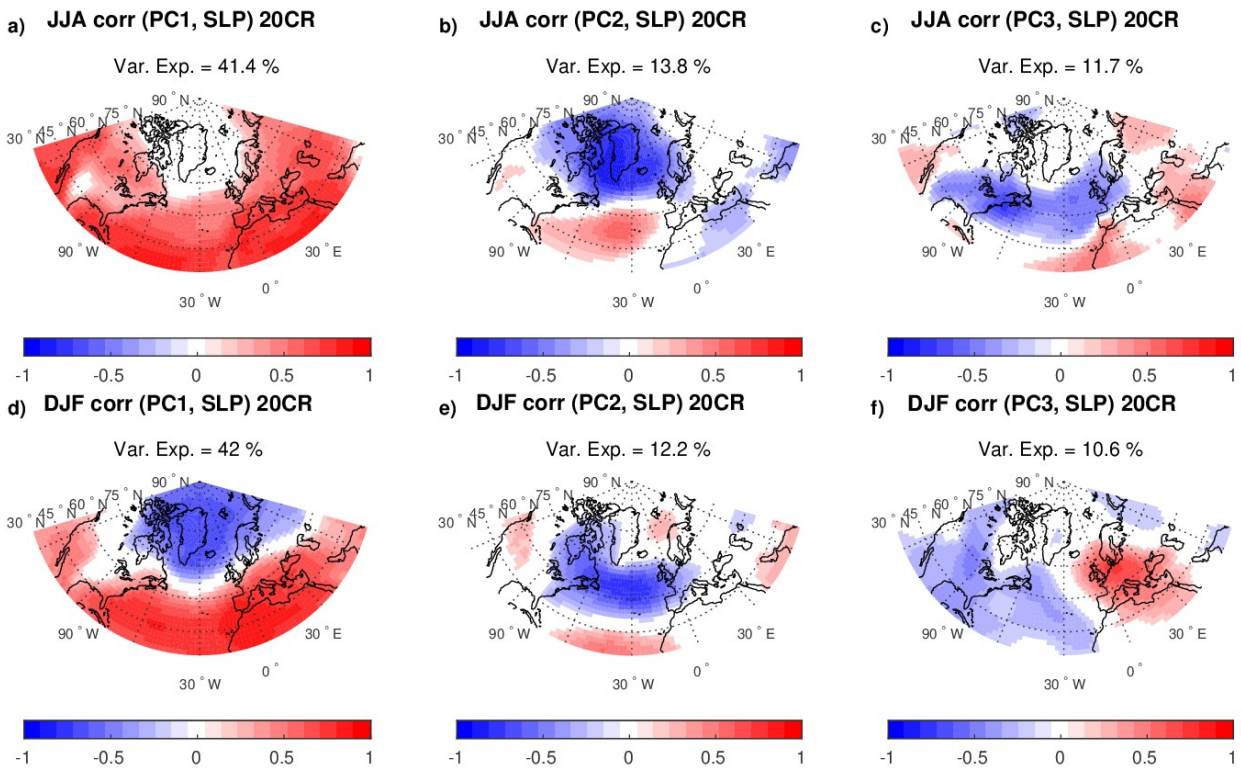

Figure S11: a)-c) regression of the first three 20CR PCs of SLP on 20CR JJA SLP, which corresponds to the EOF patterns. Top d)-f) same as a)-c), but for DJF. The time period is 1851-1970. Only data shown for $p<0.05$.

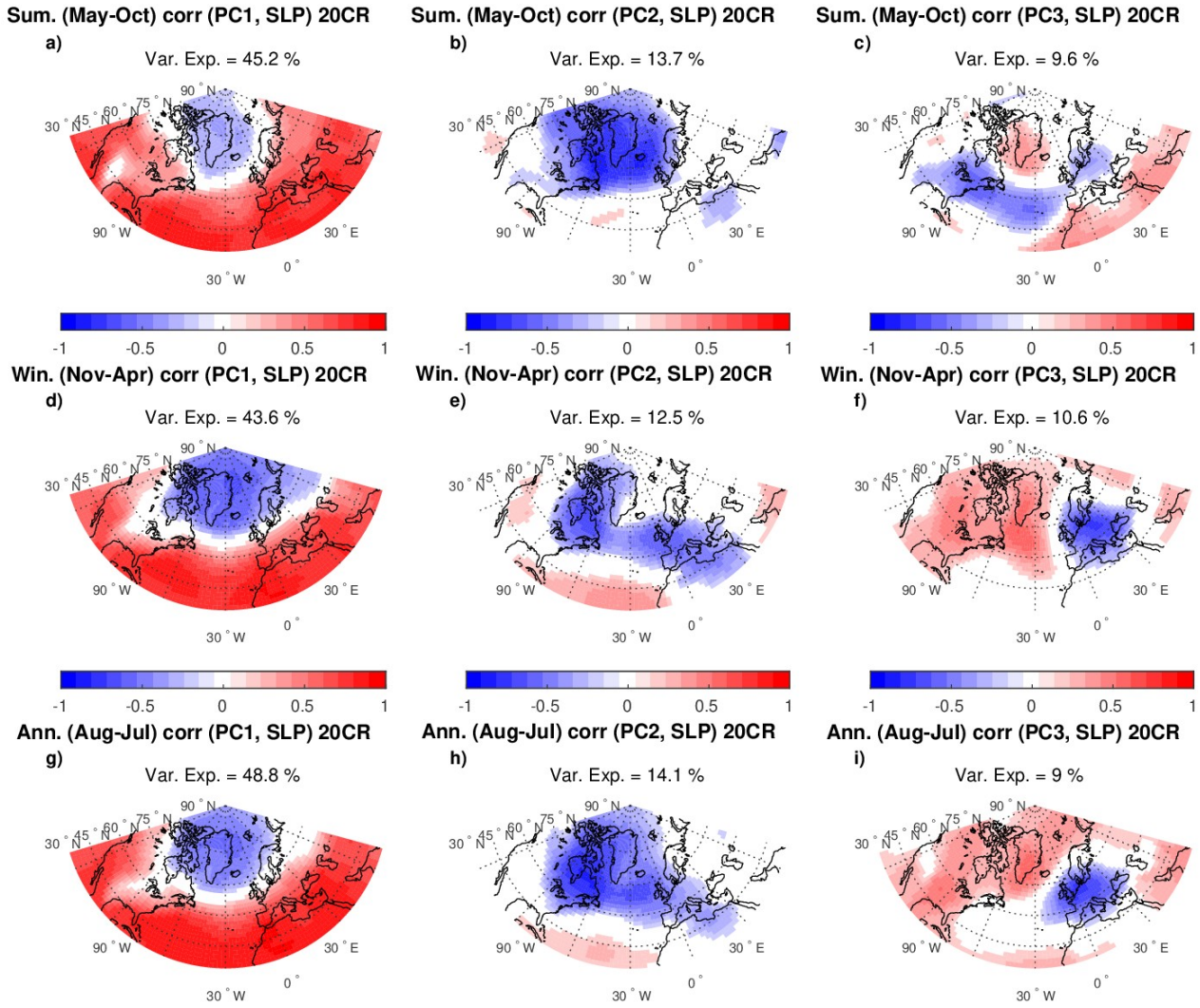

Figure S12: a)-c) regression of the first three 20CR PCs of SLP on 20CR sum50 (May-Oct) SLP, which corresponds to the reconstructed EOF patterns. d)-f) same as a)-c), but for Win50 (Nov-Apr). g)-i) same as a)-c), but for the winter centered annual mean (Win100, Aug-Jul). The time period is 1851-1970. Only data shown for $p<0.05$.

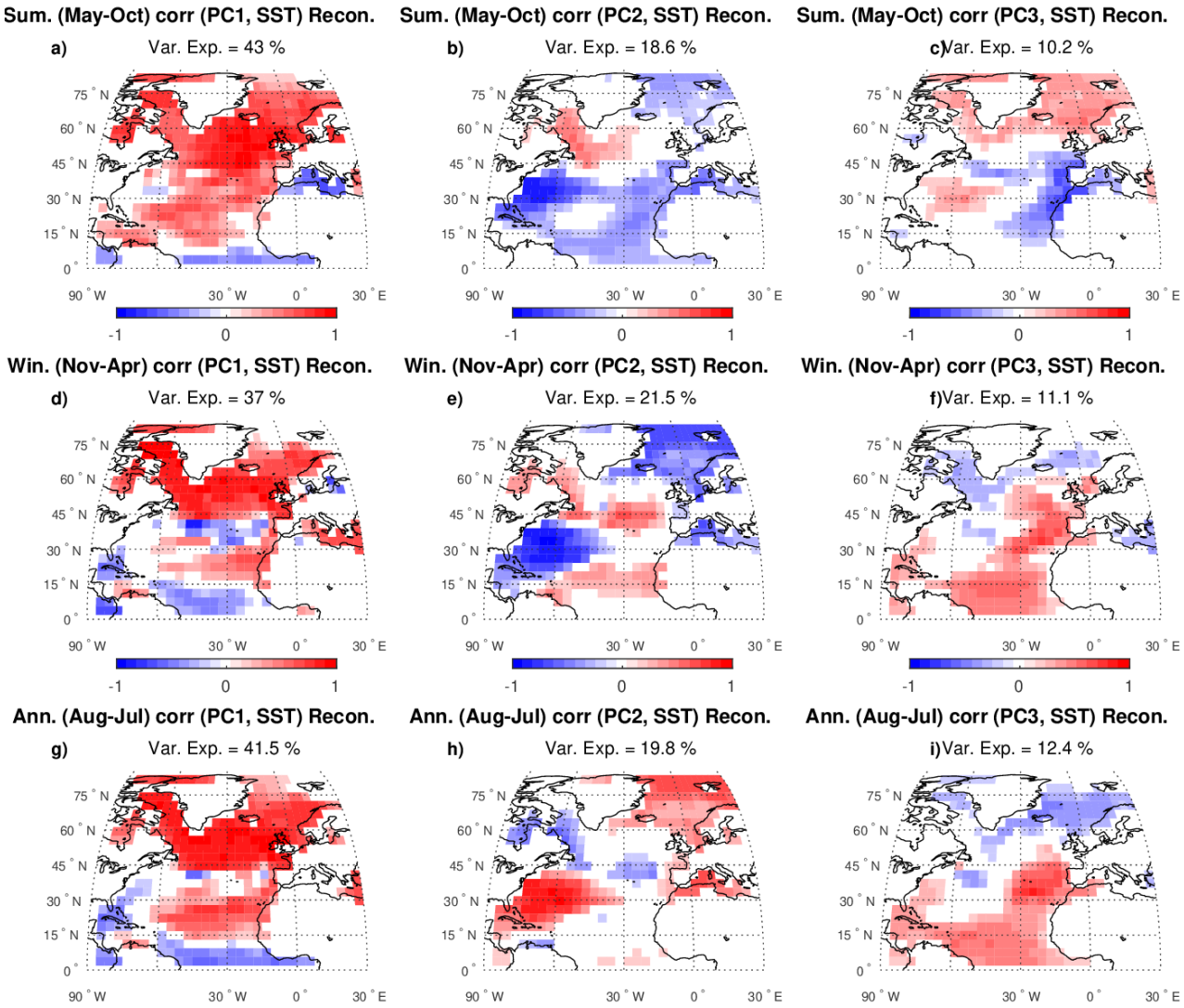

Figure S13: a)-c) regression of the first three reconstructed PCs of SSTs on reconstructed Sum50 SSTs, which corresponds to the reconstructed EOF patterns. d)-f) same as a)-c), but for Win50. g)-i) same as a)-c), but for the reconstructed winter centered annual mean (Win100, Aug-Jul). The time period is 1851-1970. Only data shown for $p < 0.05$.

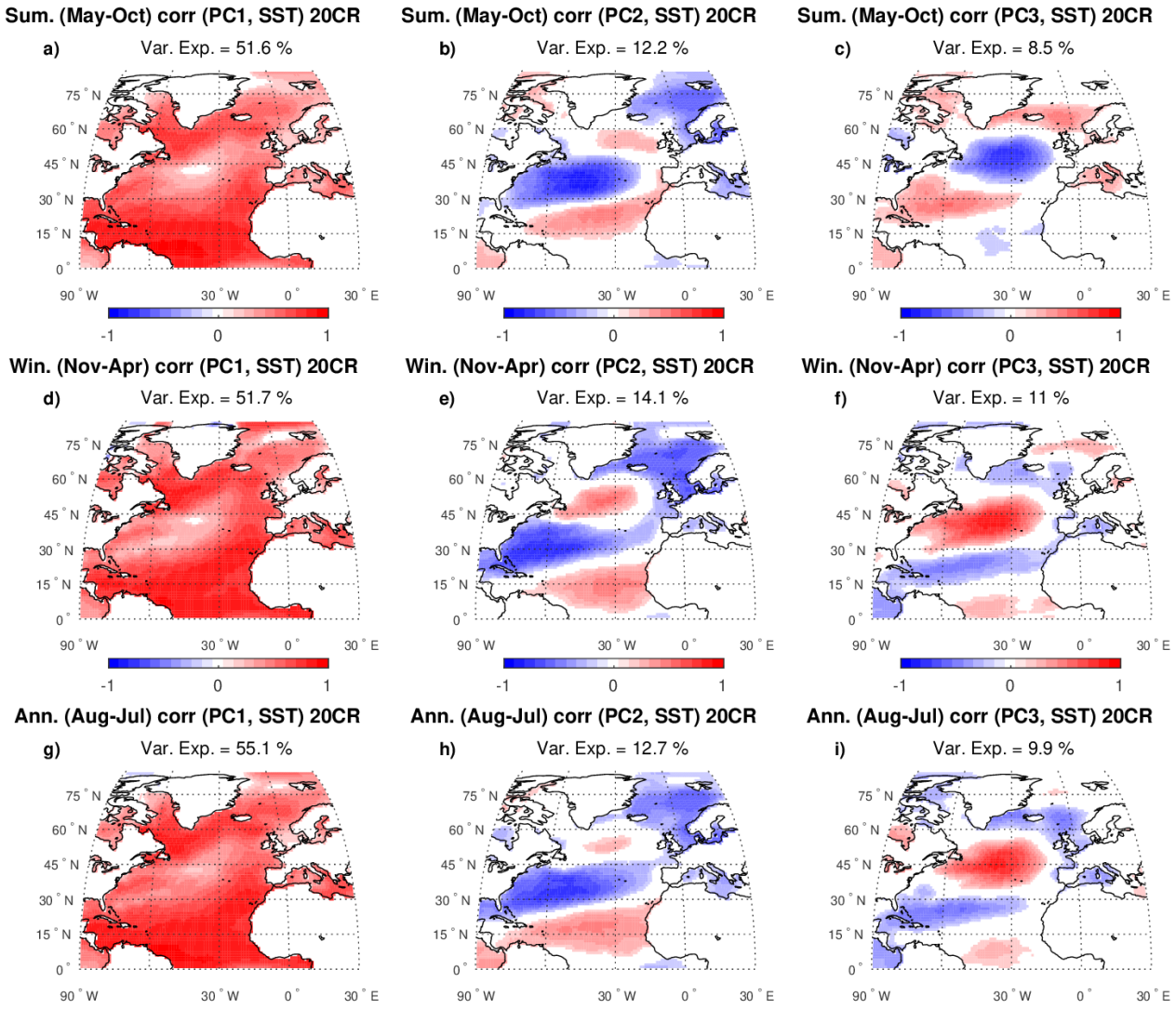

Figure S14: a)-c) regression of the first three COBE SST PCs on COBE sum50 (May-Oct) SSTs, which corresponds to the reconstructed EOF patterns. d)-f) same as a)-c), but for Win50 (Nov-Apr). g)-i) same as a)-c), but for the winter centered annual mean (Win100, Aug-Jul). The time period is 1851-1970. Only data shown for $p<0.05$.